EPJ Web of Conferences **303**, 01014 (2024) https://doi.org/10.1051/epjconf/202430301014
MENU 2023

Search for Hybrid Mesons at GlueX

William Imoehl[1,*]
on behalf of the GlueX Collaboration

[1]Carnegie Mellon University, Pittsburgh, PA

Abstract.
Recent lattice QCD calculations predict a multiplet of hybrid mesons, which are mesons with gluonic degrees of freedom. By mapping out the hybrid meson spectrum, we can gain insight into how the gluon contributes to the properties of bound states in QCD. The $\pi_1(1600)$ is a candidate for the lightest hybrid meson. This state has exotic quantum numbers of $J^{PC} = 1^{-+}$, which are forbidden for conventional mesons. The GlueX experiment has collected high statistics photoproduction data, which we are using to search for the $\pi_1(1600)$. These proceedings will summarize the search strategy for the $\pi_1(1600)$ at GlueX, including the most recent results in the $\omega\pi\pi$, $\eta\pi$, and $\eta'\pi$ final states.

1 Introduction

One of the fundamental goals of nuclear and particle physics is to understand the types of bound states that are allowed in QCD. The simplest bound states of mesons ($q\bar{q}$) and baryons (qqq) have been heavily studied, but more complicated quark configurations are also allowed. Hybrid mesons are $q\bar{q}$ bound states with gluonic excitations. They are particularly interesting because their spectrum gives information on how the gluon contributes to the properties of bound states in QCD, a key open question in hadronic physics. Several predicted hybrid mesons have J^{PC} values that are not possible for conventional mesons. These spin-exotic states have a unique experimental signature and cannot mix with conventional mesons.

The study of hybrid mesons has been quite active in recent years. Lattice QCD has predicted the spectrum of light mesons, including possible hybrid states [1]. Included in this spectrum is a nonet of spin-exotic $J^{PC} = 1^{-+}$ hybrid mesons, the lightest of which is predicted to be an isospin-1 state. This state likely corresponds to the $\pi_1(1600)$, which has been seen by multiple experiments. In addition, BESIII has recently observed the $\eta_1(1855)$ [2], which is a candidate for either the η_1 or η_1' hybrid meson predicted by lattice QCD.

The most recent experimental results for the $\pi_1(1600)$ come from the Joint Physics Analysis Center (JPAC) analysis [3] of the $\eta^{(\prime)}\pi$ $P-$wave intensities from COMPASS [4]. The measured $\eta\pi$ intensity has a broad peak at around 1.4 GeV/c^2, while the $\eta'\pi$ intensity has a narrower peak near 1.6 GeV/c^2. Historically, these peaks were assumed to be independent of one another, so there was both a $\pi_1(1400)$ candidate in $\eta\pi$ and a $\pi_1(1600)$ candidate in $\eta'\pi$. This presented a problem, since lattice QCD only predicts a single isovector $J^{PC} = 1^{-+}$ hybrid meson below 2 GeV/c^2. This issue was resolved by JPAC when they performed a simultaneous fit to both the $\eta\pi$ and $\eta'\pi$ distributions. They find that both distributions can

*e-mail: wimoehl@jlab.org

be described by a single resonance with a mass of $1564 \pm 24 \pm 86$ MeV/c^2 and a width of $492 \pm 54 \pm 102$ MeV [3].

2 The GlueX Experiment

The GlueX experiment uses a linearly polarized photon beam that is produced via the coherent bremsstrahlung process from an electron beam impinging on a thin diamond radiator. These photons are incident on a liquid hydrogen target, which can produce mesons via $-t$ channel exchange processes. The nearly hermetic GlueX detector can detect both charged and neutral particles, which allows our experiment to reconstruct relatively complicated final states. The GlueX Phase-1 data taking was finished in 2018, and comprises approximately 250 billion events. All analyses shown in this document use the Phase-1 data set. A detailed description of the experimental apparatus can be found in Ref. [5].

3 $\pi_1(1600)$ Photoproduction Cross Section Limit

Recent lattice QCD predictions suggest the $\pi_1 \to b_1\pi$ decay mode will be dominant, with a branching fraction between 69.5% and 100% [6]. Since b_1 decays to $\omega\pi$, this means the $\omega\pi\pi$ final state could have a sizable π_1 signal. The b_1 is broad and the decay $\pi_1 \to b_1\pi$ will be dominantly $S-$wave, so extracting this signal from the $\omega\pi\pi$ system will be difficult. Instead of performing the partial-wave analysis to this system, we instead use it to set upper limits on the photoproduction cross section of the $\pi_1^0(1600)$ and $\pi_1^-(1600)$. Previous results from CLAS set an upper limit of $\sigma(\gamma p \to \pi_1^+ n) < 13.5$ nb [7] for photon beam energies between 4.8 and 5.4 GeV. These new upper limits on $\pi_1^0(1600)$ and $\pi_1^-(1600)$ photoproduction from GlueX are the first limits for the negatively charged and neutral $\pi_1(1600)$ states, and they cover the photon beam energy range of 8 to 10 GeV.

GlueX has recently measured the cross sections for the processes $\gamma p \to \omega\pi^+\pi^- p$, $\gamma p \to \omega\pi^0\pi^0 p$, and $\gamma p \to \omega\pi^-\pi^0\Delta^{++}$ for $0.1 < -t < 0.5$ (GeV/c)^2, where $-t$ is the squared four-momentum transfer to the recoil baryon. Note that the $\pi_1(1600)$ is an isospin-1 state, so to enhance our sensitivity, we want to isolate just the isospin-1 components of the $\omega\pi\pi$ cross sections. Assuming there are no isospin-2 (flavor-exotic) contributions, the $\omega\pi^+\pi^-$ distributions have both isospin-1 and isospin-0 components, while $\omega\pi^0\pi^0$ is purely isospin-0. Using Clebsch-Gordan coefficients, we can use these two distributions to separate out the neutral isospin-1 cross section:

$$\sigma(\omega\pi\pi)_{I=1} = \sigma(\omega\pi^+\pi^-) - 2\sigma(\omega\pi^0\pi^0). \tag{1}$$

For the case of $\omega\pi^-\pi^0$, only isospin-1 contributions are allowed.

The measured isospin-1 cross sections for $\omega\pi\pi$ are shown in Figure 1. There is no obvious $\pi_1(1600)$ signal, so we use these distributions to set an upper limit on the cross sections $\sigma(\gamma p \to \pi_1^0(1600)p)$ and $\sigma(\gamma p \to \pi_1^-(1600)\Delta^{++})$. We do this by only including contributions from the $a_2(1320)$ and $\pi_1(1600)$, which allows us to find the largest $\pi_1(1600)$ cross section that is consistent with our data. The $a_2(1320)$ shape comes from the PDG [8], and the size is fixed based on the measured cross section from $\eta\pi$ partial-wave analyses, where non-resonant contributions are more accurately modeled. The $\pi_1(1600)$ shape is based on the JPAC parameters from Ref. [3], and the size of this component is allowed to float. We only fit the $1.2 < M(\omega\pi\pi) < 1.6$ GeV/c^2 mass region, since extending to higher masses would require adding a background shape, which would add a model dependence to our limit.

Based on these fits to the isospin-1 cross sections and the relevant $\mathcal{B}(a_2(1320) \to \omega\pi\pi)$ and $\mathcal{B}(\pi_1(1600) \to b_1\pi)\mathcal{B}(b_1 \to \omega\pi)$, we find the $\pi_1(1600)$ cross section upper limit is the

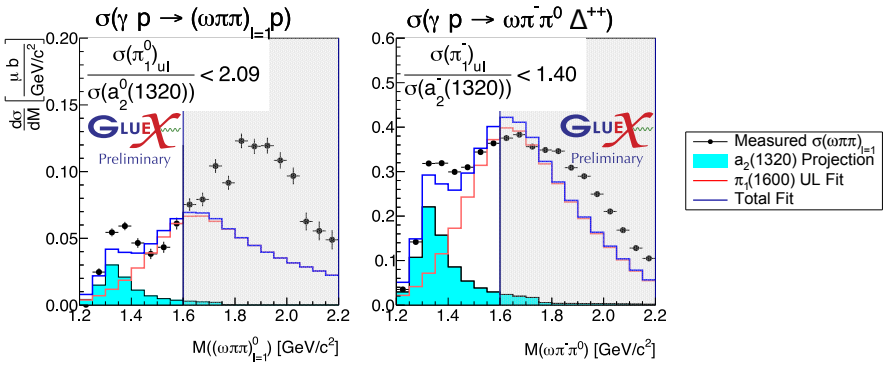

Figure 1. Measured isospin-1 $\omega\pi\pi$ cross sections and fits used to determine the upper limit on the $\pi_1(1600)$ photoproduction cross section.

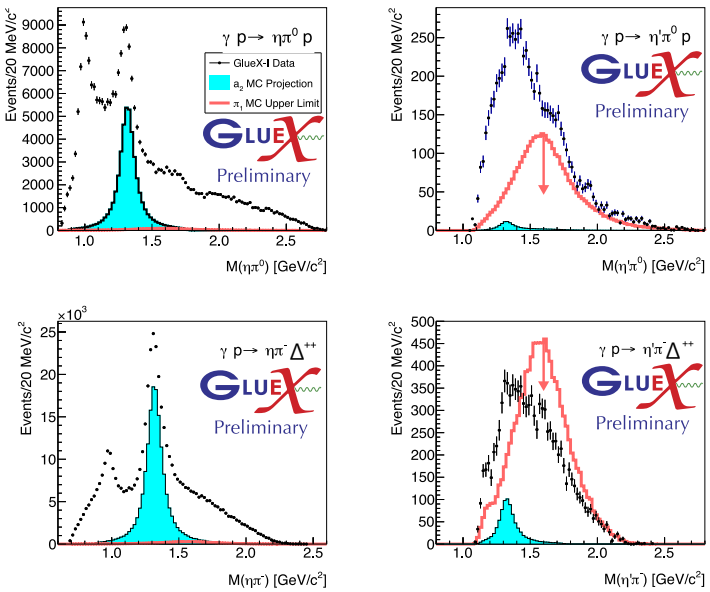

Figure 2. Measured $\sigma(a_2(1320))$ and $\sigma_{ul}(\pi_1(1600))$ projected to the $\eta\pi$ and $\eta'\pi$ final states.

same order of magnitude as the measured $a_2(1320)$ cross sections. We combine this result with the predicted π_1 decay widths to $\eta^{(\prime)}\pi$ from lattice QCD, which allows us to test our discovery potential in these final states at GlueX. These results are shown in Figure 2. We find that for $\eta\pi$, the $\pi_1(1600)$ will be no more than a percent-level contribution, while for $\eta'\pi$, we cannot rule out the $\pi_1(1600)$ being the dominant feature.

4 $\eta\pi$ Partial-Wave Analyses

The golden channels for searching for the $\pi_1(1600)$ are the $\eta\pi$ and $\eta'\pi$ decays, since contributions to the odd partial-waves correspond to J^{PC} values that are not allowed for conventional

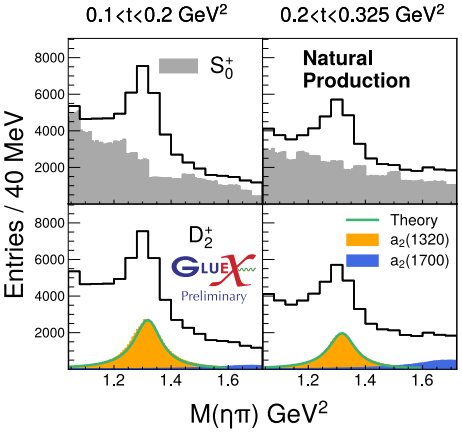

Figure 3. Partial-wave analysis of the $\gamma p \to \eta\pi^0 p$ process, showing the S_0^+ (top) and D_2^+ (bottom) contributions for two $-t$ bins.

mesons. For both $\eta\pi$ and $\eta'\pi$, we expect a contribution from the $a_2(1320)$. The contribution is much larger in the $\eta\pi$ distribution, so measuring the size, shape, and production of the $a_2(1320)$ in $\eta\pi$ can help constrain the results in the $\eta'\pi$ analysis. The $a_2(1320)$ is expected to interfere with the $\pi_1(1600)$ signal, so a thorough understanding of the $a_2(1320)$ shape is necessary for our search for the $\pi_1(1600)$.

GlueX uses a polarized photon beam, and this polarization information allows us to separate out different production processes. Mesons are generally produced through $-t$ channel reactions at our photon beam energies. We distinguish between natural ($\eta = +1$) exchange particles with $J^P = 0^+, 1^-, 2^+$, and unnatural ($\eta = -1$) exchange particles with $J^P = 0^-, 1^+, 2^-$. Our partial-wave analyses incorporate the naturality of the exchange particle, so we are able to distinguish between natural and unnatural exchanges.

We use this partial-wave analysis (PWA) framework to study the $\eta\pi^0$ system. The dominant states we expect to contribute are the $a_2(1320)$ and $a_2(1700)$, which will appear in the $D-$wave. Ultimately, we want a mass independent PWA, but this fit has many free parameters that can lead to fitting instabilities. Since the $a_2(1320)$ and $a_2(1700)$ are the main contributions and they are well separated, we add in physical constraints by modeling both states as Breit-Wigners. Example fits for two bins of $-t$ are shown in Figure 3. The fit shows the S_0^+-wave has no obvious resonant contributions, while the $a_2(1320)$ (orange) and $a_2(1700)$ (blue) have clear contributions in the D_2^+-wave.

This fit is repeated in bins of $-t$, which allows us to measure the differential $a_2(1320)$ cross section as a function of $-t$, as shown in Figure 4. In addition to the measured cross section values, we also show the components that come from natural and unnatural parity exchange. This is the first separation of the natural and unnatural parity exchanges for the $a_2(1320)$, which comes from the polarization information at GlueX. Also shown in the plot are theory predictions for the size and shape of the $a_2(1320)$ cross section, provided by a JPAC model that was fit to unpolarized CLAS data at lower energies [9]. The overall shape of the measured cross section agrees well with the theoretical predictions.

We also want to measure the cross section for the $a_2^-(1320)$ in the $\gamma p \to \eta\pi^-\Delta^{++}$ reaction. The fits use the same procedure as $\eta\pi^0$, and an example fit is shown in Figure 5. In this case, we find almost no S_0^--wave contributions and a large $a_2^-(1320)$ signal in the D_1^--wave.

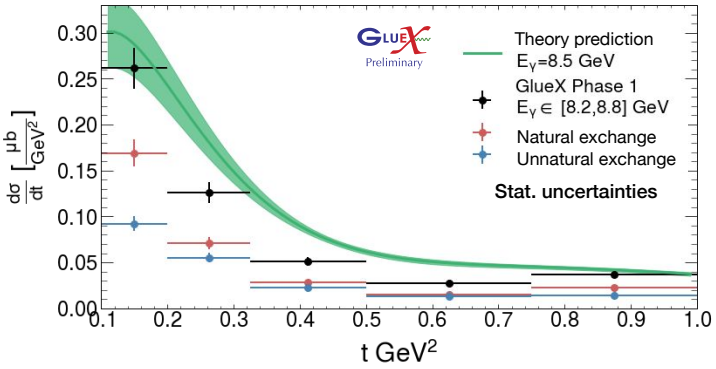

Figure 4. Measured differential $a_2^0(1320)$ cross section as a function of $-t$.

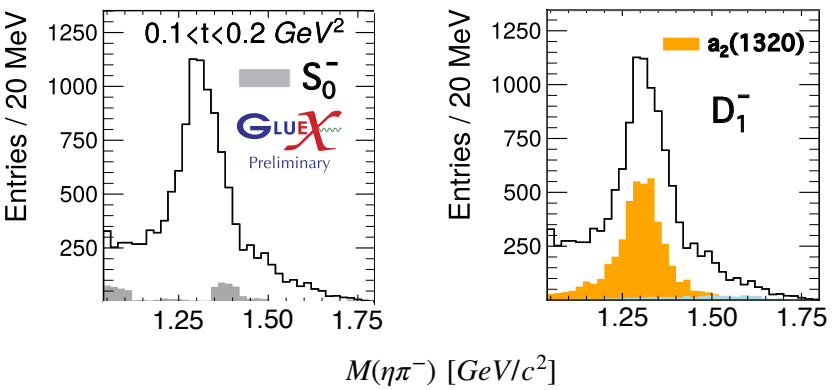

Figure 5. Partial-wave analysis of the $\gamma p \to \eta\pi^-\Delta^{++}$ process, showing the S_0^--wave and D_1^--wave components.

The $\gamma p \to \eta\pi^-\Delta^{++}$ reaction has an added complication due to the unstable recoil baryon. There can be background under the $\Delta^{++} \to \pi^+ p$ candidates, which must be modeled in order to get an accurate measurement of $\sigma(\gamma p \to a_2^-(1320)\Delta^{++})$. We are working with colleagues at JPAC on modeling this background in the fit. What we learn from modeling the Δ^{++} background here can be used when we ultimately study $\gamma p \to \eta'\pi^-\Delta^{++}$ process, where we expect our best sensitivity to the $\pi_1^-(1600)$.

5 Prospects for $\eta'\pi$ Analyses

Our upper limits on the $\pi_1(1600)$ photoproduction cross section show the $\pi_1(1600) \to \eta'\pi$ decay has the best discovery potential. When COMPASS performed their $\eta'\pi$ partial-wave analysis [4], they saw a clear forward-backward asymmetry in $\cos\theta_{GJ}$, which is indicative of interference between even and odd partial-waves. We compare their plots of $\cos\theta_{GJ}$ versus $M(\eta'\pi^-)$ to the same distributions in the GlueX data in Figure 6. Note that these figures do not have acceptance corrections, and contributions from the double Regge process and baryon

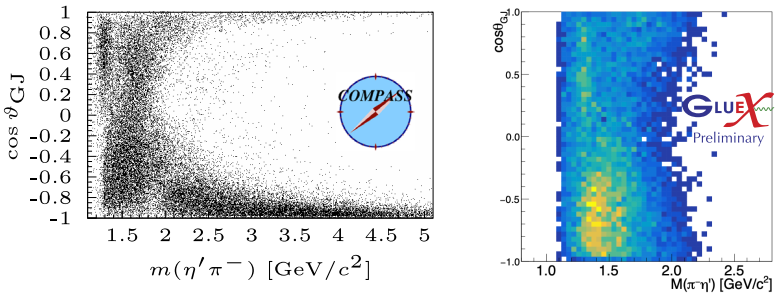

Figure 6. Plots of $\cos\theta_{GJ}$ as a function of $M(\eta'\pi^-)$ for COMPASS (left) and GlueX (right). There is a similar forward-backward asymmetry in the two distributions.

backgrounds need to be fully understood. With these caveats, there is a striking similarity in the forward-backward asymmetry in $\cos\theta_{GJ}$. We are working on performing a moment analysis to more rigorously probe the potential exotic signal in our $\eta'\pi^-$ distributions.

6 Summary

GlueX has a unique photoproduction data set that we are using to search for hybrid mesons. We have set the first upper limits on the $\pi_1^0(1600)$ and $\pi_1^-(1600)$ photoproduction cross sections. We have also used those limits to project our sensitivity into the $\eta\pi$ and $\eta'\pi$ final states. We are performing partial-wave analyses on the $\eta\pi$ systems, and have measured the differential $a_2^0(1320)$ cross section as a function of $-t$. Work is ongoing on the other $\eta^{(\prime)}\pi$ channels.

References

[1] Jozef J. Dudek, Robert G. Edwards, Peng Guo, and Christopher E. Thomas, (Hadron Spectrum Collaboration), Phys. Rev. D, **88** 094505 (2013).
[2] M. Ablikim *et al.* (BESIII Collaboration), Phys. Rev. Lett. **129** 192002 (2022).
[3] A. Rodas *et al* (JPAC), Phys. Rev. Lett., **122** 042002 (2019).
[4] C. Adolph, *et al.* (COMPASS Collaboration), Phys. Lett. B, **740** 303-311 (2015).
[5] S. Adhikari *et al.* (GlueX Collaboration), Nuclear Inst. and Methods in Physics Research, A **987** 164807 (2021).
[6] Antoni J. Woss, and Jozef J. Dudek, and Robert G. Edwards, and Christopher E. Thomas, and David J. Wilson, (Hadron Spectrum Collaboration), Phys. Rev. D **103** 054502 (2021).
[7] M. Nozar *et al.* (CLAS Collaboration), Phys. Rev. Lett. **102** 102002 (2009).
[8] P.A. Zyla et al. (Particle Data Group), Prog. Theor. Exp. Phys. 2020, 083C01 (2020)
[9] V. Mathieu *et al.* (JPAC), Phys. Rev D. **102** 014003 (2020).